EPJ manuscript No.
(will be inserted by the editor)

Structure and Optic Response of the Na_9^+ and Na_{55}^+ Clusters

S. Kümmel[1], P.-G. Reinhard[2], and M.Brack[1]

[1] Institute for Theoretical Physics, University of Regensburg, D-93040 Regensburg, Germany
(stephan.kuemmel/matthias.brack@physik.uni-regensburg.de)
[2] Institute for Theoretical Physics, University of Erlangen, D-91077 Erlangen, Germany
(reinhard@theorie2.physik.uni-erlangen.de)

Received: / Revised version:

Abstract. We present the ionic geometries of Na_9^+ and Na_{55}^+ clusters obtained in the "cylindrically averaged pseudopotential scheme". Our structures are tested by calculating photoabsorption spectra and comparing them to the experimentally measured ones. We employ a local pseudopotential that has been constructed to reproduce atomic and bulk properties of sodium. Comparing the results using different pseudopotentials, we find that the position of the dipole resonance is greatly influenced by details of the pseudopotentials, showing that these must be used consistently both in the geometry optimization and the calculation of the optic response.

PACS. 36.40.-c Atomic and molecular clusters – 31.15.-p Calculations and mathematical techniques in atomic and molecular physics – 71.15.-m Methods of electronic structure calculations

Since the discovery of shell effects in free sodium clusters [1], there has been a great interest in the structure of these particles. Theoretical investigations based on the jellium model (see, e.g., Refs. [2–5]) could explain several experimentally observed features qualitatively. However, many aspects of modern cluster physics result from the interplay of electronic and ionic degrees of freedom, and a more realistic description of metal clusters is necessary. The most sophisticated approach is given by quantum chemical all-electron methods. But due to their computational expense they are restricted to clusters consisting of only a few atoms [6]. A considerable simplification can be obtained by treating only valence electrons explicitly and describing core electrons and nucleus by a pseudopotential. Geometry optimization in three dimensions using the Car-Parrinello scheme [7,8] or gradient methods [9,10] is, however, still such a complex task that to our knowledge the only *ab intio* study of a sodium cluster with more than twenty electrons is the recent work of Rytkönen *et al.* [11]. But larger clusters are of interest due to new experiments [12] and for the investigation of the onset of volume effects [13].

Among the approximations that have been developed to study ionic effects in larger clusters are for example the "spherically averaged pseudopotential scheme" (SAPS) [14], extensions of the Hückel model [15] and pseudopotential perturbation theory [16]. With the "cylindrically averaged pseudopotential scheme" (CAPS) [17] we use a method that is less restrictive than SAPS and goes beyond the perturbation approaches since it allows for a free geometry optimization. The basic idea of CAPS is to simultaneously solve the equations

$$\frac{\partial E}{\partial \mathbf{R}} = 0 \qquad \frac{\delta E}{\delta n} = 0 \tag{1}$$

self-consistently. For a cluster with electronic density n, ionic positions $\mathbf{R}$ and N ions with Z valence electrons each, the energy functional E is given by

$$E[n;\mathbf{R}] = T_s[n] + E_{xc}[n] + \frac{e^2}{2}\int\int \frac{n(\mathbf{r})n(\mathbf{r}')}{|\mathbf{r}-\mathbf{r}'|}\,d^3r'\,d^3r + \int n(\mathbf{r})V_{ei}(\mathbf{r};\mathbf{R})\,d^3r + \frac{Z^2e^2}{2}\sum_{\substack{i,j=1\\ i\neq j}}^{N}\frac{1}{|\mathbf{R}_i-\mathbf{R}_j|}. \tag{2}$$

The electronic problem is solved via the Kohn-Sham equations in the local density approximation (LDA) with the exchange-correlation functional of Perdew and Wang [18]. The optimal ionic geometry is searched for without any constraint, and in order to reduce the problems resulting from the strong isomerism found in sodium clusters, we employ the method of simulated annealing.

This scheme can be used to calculate structures of large clusters due to two approximations which are made in the evaluation of the energy functional (2). The first is that we describe the interaction between valence electrons and ions by a local pseudopotential. This point has already been discussed in [19], and we will come back to it below. The second is that while the ions are treated fully three-dimensionally, the electronic density is restricted to cylindrical symmetry, i.e., $V_{ps}(|\mathbf{r}-R_i|)$ is replaced by its cylindrical average

$$\bar{V}_{\mathrm{ps}}(z,\rho;z_i,\rho_i)=\frac{1}{2\pi}\int_0^{2\pi}V_{\mathrm{ps}}(|\mathbf{r}-R_i|)\,d\varphi. \tag{3}$$

Certainly the second approximation is a far reaching one. But since the photoabsorption spectra of singly charged sodium clusters suggest that most of these clusters are of overall axially symmetric shape [20,21], it does not seem unreasonable. Also, one can hope that with growing cluster size – and CAPS is designed for clusters with several tens of atoms – strong triaxial deformations will hardly occur. On the other hand, an approximation cannot be accepted without checking its consequences. Therefore, we perform checks in two ways. First, where available, we compare cluster geometries obtained in CAPS to geometries obtained with three dimensional methods. Second, by computing the photoabsorption spectra for our CAPS clusters and comparing with the experimentally measured ones, we can get at least a qualitative check for our results. But before we present some results we want to add a few remarks about the local pseudopotential.

The potential that a valence electron experiences from one ion contains contributions from the nucleus and the core electrons. These contributions can be put together into an effective potential, the so-called pseudopotential. In general, such a pseudopotential will be nonlocal in the sense that each angular momentum component of the valence electron wavefunction feels a different potential. This is a consequence of the requirement that valence and core wavefunctions must be orthogonal to each other. But a sodium atom has a rather simple electronic structure with one $3s$ electron added to otherwise completely filled shells, resulting in a pseudopotential that is effectively local. Therefore, the simplest possible pseudopotentials, e.g., the Ashcroft empty-core potential and related parametrizations, have been used in many theoretical studies of sodium clusters [14,16,17]. These pseudopotentials were constructed such that only few bulk properties were matched. However, as demonstrated in [19] and Fig. 1 below, pseudopotentials sensitively influence the position of the calculated dipole resonance. It is therefore necessary to construct pseudopotentials that are close to the real ionic potential. At the same time, one wants to stay with a local pseudopotential and build it such that it can be used easily in numerical calculations. To this end we have constructed a pseudopotential with the parametrization

$$V_{\mathrm{Gauss}}(r)=-\frac{Ze^2}{r}\left\{c_1\,\mathrm{erf}\left(\frac{r}{\sqrt{2}\sigma_1}\right)+c_2\,\mathrm{erf}\left(\frac{r}{\sqrt{2}\sigma_2}\right)\right\}. \tag{4}$$

It fulfills the last requirement since it leads, via Poisson's equation, to a Gaussian pseudo-density that can efficiently be handled numerically in real space. But the important step that turns (4) into a valid pseudopotential is the careful choice of the parameters $c_1, c_2, \sigma_1, \sigma_2$. Since clusters are bridging the region between the single atom and the bulk, a valid pseudopotential must reproduce the most important properties of both these two limiting cases. For the bulk, we chose the Wigner-Seitz radius r_s and the compressibility B as the relevant quantities, for the atom the energy e_{a} of the $3s$ level. These characterize a metal and at the same time influence electronic excitations, either directly or via the volume of the crystal or the cluster, respectively. Therefore, it is important that a pseudopotential to be used for calculations of ionic structures and electronic excitations gives correct values for the above quantities. We achieve this for the parametrization (4) by choosing c_1, σ_1 and σ_2 such that the experimental values $r_{\mathrm{s}} = 3.93\,\mathrm{a}_0$ and $B = 0.073\,\mathrm{Mbar}$ are reproduced in a second-order perturbation theory calculation [19,22], and that the experimental value [23] $e_{\mathrm{a}} = 0.378\,\mathrm{Ry}$ is matched within 1%. The remaining parameter c_2 is fixed by the condition $Z = 1$. Our final set of parameters is

$$\sigma_1 = 0.681\,\mathrm{a}_0, \qquad c_1 = -2.292, \tag{5}$$

$$\sigma_2 = 1.163\,\mathrm{a}_0, \qquad c_2 = 3.292. \tag{6}$$

The physical properties of the resulting pseudopotential are the same as for the one give in [19], but the present one has the advantage of being smoother and thus easier to handle numerically on a grid.

On the basis of this pseudopotential, we have calculated the ionic structure for a wide range of cluster sizes with CAPS. Here we first discuss Na_9^+, because it allows us to demonstrate the possibilities and limitations of our approach. Due to its smallness, Na_9^+ can be studied with three-dimensional *ab initio* methods, and its structure is therefore well known. Quantum chemical calculations [6] find three close-lying isomers with C_{2v}, D_{4d} and $C_{4v} \to C_{2v}$ symmetry. The right panel of Fig. 1 shows the ground-state geometry which we find with CAPS. It is extremely close to the three-dimensional $C_{4v} \to C_{2v}$ structure, that is also found as the ground-state in three-dimensional density functional calculations [28], demonstrating the capability of CAPS to describe even small systems in a good approximation. However, a small error comes from the cylindrical averaging: in CAPS, the two squares of four atoms have the same edge length, whereas the three-

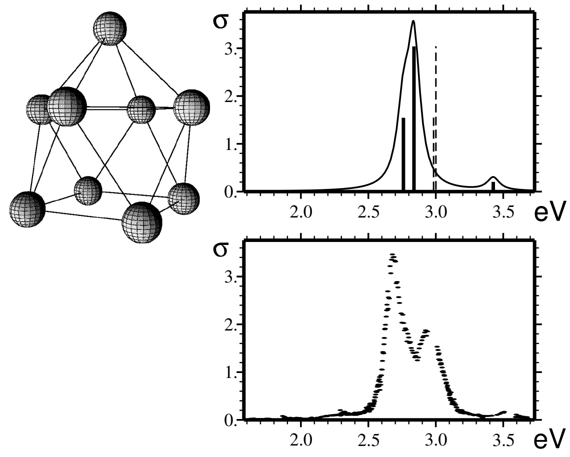

Fig. 1. Lower right panel: Experimental photoabsorption cross section σ of Na_9^+ [24]. Left panel: CAPS geometry of Na_9^+. Upper right panel: LRPA spectrum for the CAPS geometry (see text for details).

dimensional calculation shows the lower square with a slightly shorter edge than the upper. In the left panel of Fig. 1, the dots represent the photoabsorption cross section of Na_9^+ measured at T=105 K [24]. The vertical lines show the percentages of the energy-weighted dipole sum rule, i.e., the percentages of the oscillator strength (in arbitrary units), against energy (in eV), calculated in the "localized random phase approximation" (LRPA) [4,25]. The full lines, which were folded with a Lorentzian line of width 0.11 eV to simulate the actual widths, were obtained for the Na_9^+ geometry shown in the right panel, i.e., with the pseudopotential introduced above. The dashed lines result from a calculation where the empty-core like pseudopotential of [17] was used for both the structure optimization and the photoabsorption spectrum. One clearly sees that first, the dipole resonance depends on the pseudopotential, and second, that the rigorously constructed pseudopotential gives a lower resonance energy which is in better agreement with experiment than the one from the empty-core like pseudopotential. This explains why earlier calculations based on the empty-core like version [26,27] found a considerable blue shift of the dipole resonance. The spectrum calculated with our pseudopotential shows a splitting of the main transition and correctly reproduces the small subpeak around 3.5 eV. However, the relative heights of the main transitions are reversed with respect to the experiment. An explanation for this might be the fact that the LRPA is tailored to describe collective excitations and is less suited to describe situations where selective particle-hole states interfere with a collective resonance. It is currently assumed that such a mechanism contributes to the splitting observed in the resonance of Na_9^+ at low temperature [28]. Also, it should be noticed that even the sophisticated methods of quantum chemistry predict relative peak heights that are not in agreement with the experiment[6,9], hinting at that other isomers might also be part of the explanation. In summary, one can say that although CAPS and LRPA will not give all the fine details that are accessible with three-dimensional *ab initio* methods, they can very well describe the general features of a cluster.

In the following we discuss our results for Na_{55}^+. In this size range, even in our symmetry-reduced approach, we cannot be absolutely sure to have discovered all the relevant isomers. But since we found several highly symmetric geometries which are considerably lower in energy than all other structures, we have good hope that these are the important ones. The left-hand side of Fig. 2 shows two views of the CAPS geometry with the lowest energy. It can be described as a sequence of "rings" with 1,5,10,5,10,5,10,5,1 ions, where an additional ion is placed in the center of each of the decagons. The resulting valence electron density is slightly oblate. Next in energy we find structures with an electron density which is even more pronouncedly oblate, but all of these have a highest valence-electron state that is only half occupied. This might indicate that these structures would relax further when treated fully three-dimensionally. The right-hand side of Fig. 2 shows the closest stable isomer, which is higher in energy by 0.73 eV. Its electron density has a positive quadrupole and a slight octupole deformation, i.e., it is close to what an axially deformed jellium model predicts[29].

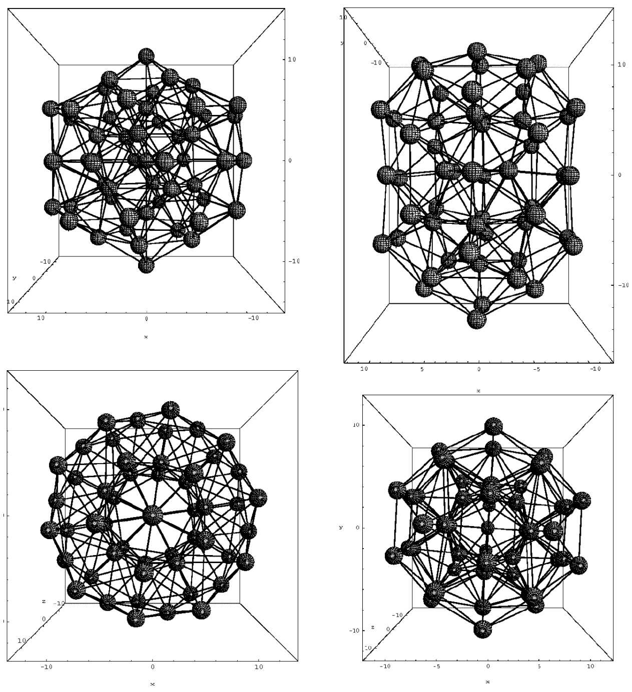

Fig. 2. Left: Side and top view of the CAPS ground-state configuration of Na_{55}^+. Right: The same views of the prolate isomer.

It is known that large sodium clusters prefer icosahedral geometries [30]. Recent experiments on the melting of sodium clusters [31] give a hint that ionic shells may also play a role in medium sized systems. Therefore, besides starting our search for the optimum ionic configuration from a random guess, we also ran a series where we started with the 55 ions arranged in an icosahedron with the nearest-neighbour spacing of bulk sodium. The results reveal that, at least in CAPS, the icosahedron is not a stable configuration for Na_{55}^+, and solving the Kohn-Sham equations with fixed ionic positions gives an energy that lies 1.16 eV above the ground-state energy.

In Fig. 3 we compare the photoabsorption spectrum of the Na_{55}^+ cluster measured experimentally [32] (top) with that obtained in our LRPA calculations for the two structures shown in Fig. 2. The configuration that we find as the ground-state gives a spectrum which is closer to the experimental one than the spectrum of the isomer, which does not show much resemblance to the experimental data. This supports the results of our structure calculations. However, three comments must be made concerning that comparison: First, the theoretical spectra show some strength in the range that was not scanned in the experiment[32]. Second, our ground-state spectrum is slightly blue shifted with respect to the experimental one.

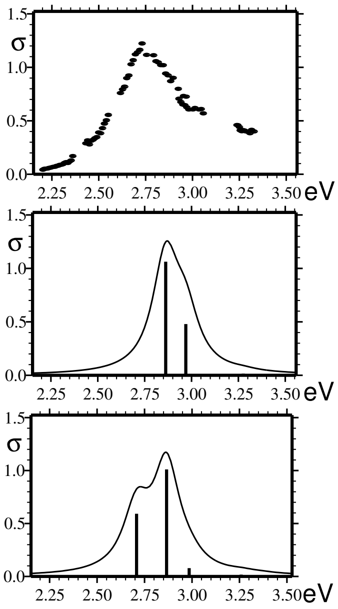

Fig. 3. Photoabsorption spectrum σ of Na_{55}^+. Top: experimental result [32]. Middle and bottom: LRPA spectra of the CAPS ground-state and of the prolate isomer, respectively (cf. Fig. 2).

And third, the high-energy shoulder is more pronounced in the experiment than in the calculations. These effects might have several causes. First, they might be due to the fact that when ionic structure is taken into account, the LRPA basis must be considerably extended compared to the basis that was sufficient for jellium model calculations. However, we have increased our basis set until we found numerical convergence; therefore the basis corrections should be small. Second, the cylindrical averaging may introduce some errors which are, however, difficult to estimate. Third, specific particle-hole excitations may play a role, as in the case of Na_9^+. Fourth, the LDA leaves room for corrections in view of the spatial variations of the electron densities (which are stronger than in jellium model calculations). Finally, the finite temperature that is present in the experiment and that we are neglecting, certainly plays a role and will shift the resonance peaks towards lower energies. In this context it is interesting to note that a slight blue shift of the dipole resonance with respect to the high-temperature experimental data has been found [33] for $Na7^+$ in a time-dependent LDA calculation. It is the aim of our future work to further investigate these effects.

We acknowledge helpful discussions with Bernd Montag and Christian Kohl. This work has been partially supported by the Deutsche Forschungsgemeinschaft.

References

1. W. D. Knight, K. Clemenger, W. A. de Heer, W. A. Saunders, M. Y. Chou und M. L. Cohen, Phys. Rev. Lett. **52**, 2141 (1984).
2. W. Ekardt, Phys. Rev. Lett. **52**, 1925 (1984).
3. D. E. Beck, Solid State Commun. **49**, 381 (1984).
4. M. Brack, Phys. Rev. B **39**, 3533 (1989).
5. B. Montag, P.-G. Reinhard, and J. Meyer, Z. Phys. D **32**, 125 (1994).
6. V. Bonačic-Koutecký, P. Fantucci, and J. Koutecký, Chem.Rev. **91**, 1035 (1991).
7. J. L. Martins, J. Buttet, and R. Car, Phys. Rev. B **31**, 1804 (1985).
8. U. Röthlisberger and W. Andreoni, J. Chem. Phys. **94**, 8129 (1991).
9. V. Bonačic-Koutecký, J. Pittner, C. Fuchs, P. Fantucci, M.F. Guest, and J. Koutecký, J. Chem. Phys. **104**, 1427 (1996).
10. A. Rubio, J.A. Alonso, X. Blase, L.C. Balbás, and S. G. Louie, Phys. Rev. Lett. **77**, 247 (1996).
11. A. Rytkönen, H. Häkkinen, and M. Manninen, Phys. Rev. Lett. **80**, 3940 (1998).
12. M. Schmidt, R. Kusche, W. Kronmüller, B. von Issendorf, and H. Haberland, Phys. Rev. Lett. **79**, 99 (1997).
13. M. Brack, Rev. Mod. Phys. **65**, 677 (1993).
14. M. P. Iñiguez, M. J. Lopez, J. A. Alonso und J. M. Soler, Z. Phys. D **11**, 163 (1989).
15. R. Poteau and F. Spiegelmann, J. Chem. Phys. **98**, 6540 (1993).
16. W.-D. Schöne, W. Ekardt and J. M. Pacheco, Phys. Rev. B **50**, 11079 (1994).
17. B. Montag and P.-G. Reinhard, Z. Phys. D **33**, 265 (1995).
18. J. P. Perdew and Y. Wang, Phys. Rev. B **45**, 13244 (1992).
19. S. Kümmel, M. Brack, and P.-G. Reinhard, Phys. Rev. B **58**, 1774 (1998).
20. W. Ekardt and Z. Penzar, Phys. Rev. B **43**, 1322, (1991).
21. J. Borggreen *et al.*, Phys. Rev. B **48**, 17507 (1993); P. Meibom *et al.*, Z. Phys. D **40**, 258 (1997); T. Hirschmann *et al.*, Z. Phys. D **40**, 254 (1997).
22. C. Fiolhais, J.P. Perdew, S.Q. Armster, J.M. MacLaren and M. Brajczewska, Phys. Rev. B **51**, 14001 (1995); Phys. Rev. B **53**, 13193(E) (1996); and references therein.
23. I. V. Abarenkov and V. Heine, Phil. Mag. **12**, 529 (1965).
24. Th. Reiners, W. Orlik, C. Ellert, M. Schmidt, and H. Haberland, Chem. Phys. Lett. **215**, 357 (1993).
25. P.-G. Reinhard, M. Brack, and O. Genzken, Phys. Rev. A **41**, 5568 (1990); P.-G. Reinhard, O. Genzken, and M. Brack, Ann. Phys. (Leipzig) **51**, 576 (1996).
26. S. Kümmel, Diploma thesis, University of Regensburg, 1997.
27. P.-G. Reinhard *et al.*, Z. Phys. D **40**, 314 (1997).
28. F. Calvayrac, P.-G. Reinhard, and E. Suraud, J. Phys. B **31**, 1367 (1998).
29. T. Hirschmann, B. Montag, and J. Meyer, Z. Phys. D **37**, 63, (1996).
30. T. P. Martin, Phys. Reports **273**, 201 (1996).
31. M. Schmidt, R. Kusche, B. von Issendorf, and H. Haberland, Nature **393**, 238 (1998).
32. M. Schmidt and H. Haberland, private communication.
33. P.-G. Reinhard, unpublished results.